• **Basic Research** •

Impact of umbelliprenin-containing niosome nanoparticles on *VEGF-A* and *CTGF* genes expression in retinal pigment epithelium cells

Farzad Dastaviz[1,2], Akram Vahidi[2], Teymoor Khosravi[3], Ayyoob Khosravi[1,4], Mehdi Sheikh Arabi[5], Abouzar Bagheri[6], Mohsen Rashidi[7], Morteza Oladnabi[1,2,8]

[1]Stem Cell Research Center, Golestan University of Medical Sciences, Gorgan 4934174516, Iran

[2]Department of Medical Genetics, School of Advanced Technologies in Medicine, Golestan University of Medical Sciences, Gorgan 4934174516, Iran

[3]Student Research Committee, Golestan University of Medical Sciences, Gorgan 4934174516, Iran

[4]Department of Molecular Medicine, Faculty of Advanced Medical Technologies, Golestan University of Medical Sciences, Gorgan 4934174516, Iran

[5]Department of Medical Nanotechnology, Faculty of Advanced Medical Technologies, Golestan University of Medical Sciences, Gorgan 4934174516, Iran

[6]Department of Clinical Biochemistry and Genetics, Faculty of Medicine, Mazandaran University of Medical Sciences, Sari 4847191628, Iran

[7]Department Pharmacology, Faculty of Medicine, Mazandaran University of Medical Sciences, Sari 4847191628, Iran

[8]Gorgan Congenital Malformations Research Center, Golestan University of Medical Sciences, Gorgan 4934174516, Iran

Correspondence to: Morteza Oladnabi. Department of Medical Genetics, School of Advanced Technologies in Medicine, Golestan University of Medical Sciences, Gorgan 4934174516, Iran. oladnabidozin@yahoo.com

Received: 2023-04-29   Accepted: 2023-09-14

Abstract

● **AIM:** To investigate the impact of niosome nanoparticles carrying umbelliprenin (UMB), an anti-angiogenic and anti-inflammatory plant compound, on the expression of vascular endothelial growth factor (*VEGF-A)* and connective tissue growth factor (*CTGF)* genes in a human retinal pigment epithelium (RPE)-like retina-derived cell line.

● **METHODS:** UMB-containing niosomes were created, optimized, and characterized. RPE-like cells were treated with free UMB and UMB-containing niosomes. The IC_{50} values of the treatments were determined using an MTT assay. Gene expression of *VEGF-A* and *CTGF* was evaluated using real-time polymerase chain reaction after RNA extraction and cDNA synthesis. Niosomes' characteristics, including drug entrapment efficiency, size, dispersion index, and zeta potential were assessed. Free UMB had an IC_{50} of 96.2 µg/mL, while UMB-containing niosomes had an IC_{50} of 25 µg/mL.

● **RESULTS:** Treatment with UMB-containing niosomes and free UMB resulted in a significant reduction in *VEGF-A* expression compared to control cells (P=0.001). Additionally, UMB-containing niosomes demonstrated a significant reduction in *CTGF* expression compared to control cells (P=0.05). However, there was no significant reduction in the expression of both genes in cells treated with free UMB.

● **CONCLUSION:** Both free UMB and niosome-encapsulated UMB inhibits *VEGF-A* and *CTGF* genes expression. However, the latter demonstrates significantly greater efficacy, potentially due to the lower UMB dosage and gradual delivery. These findings have implications for anti-angiogenesis therapeutic approaches targeting age-related macular degeneration.

● **KEYWORDS:** umbelliprenin; niosome; age-related macular degeneration; vascular endothelial growth factor-A; connective tissue growth factor

INTRODUCTION

Age-related macular degeneration (AMD) is a progressive multifactorial disorder. It is one of the major causes of blindness worldwide, affecting more than 170 million people. This number is expected to be around 300 million by 2040[1-2]. In early stage of AMD, a yellow-colored drusen deposit under the retinal pigment epithelium (RPE)

is considered as hallmark. Patients have abnormal retinal difficulties in basic visual activities like facial recognition and reading[3-4]. There are several known risk factors for the onset and progression of AMD, including aging, white ethnicity, inflammation, oxidative stress, and angiogenesis[5-8]. Vascular endothelial growth factor (VEGF) and connective tissue growth factor (CTGF) have been shown to play essential roles in regulating angiogenesis, vascular leakage, and inflammation in AMD by encouraging the formation of new blood vessels[9]. VEGF-A (located on 6p21.1 with 26 identified transcript) is the most critical factor in the angiogenesis process, which leads to an increase in the number of capillaries. As a signal protein, VEGF-A is produced by many tissues with insufficient blood circulation and functions as a part of the oxygen and nutrition delivery system[10]. Like other family members of VEGFs, it is highly conserved and considered as part of evolutionary distance between fish and mammals[11]. Among therapeutic approaches for AMD (Figure 1), VEGF inhibitors have been 'partially' successful in rehabilitating vision loss, as they are highly dependent on the efficiency of anti-VEGF agents and the patient's response[12-14]. CTGF (located on 6q23.2 with only identified transcript) belongs to the Cys-rich CCN secretory protein family, which binds to heparin. All four cysteine-rich domains of CTGF have high conservativity especially insulin-like growth factor binding protein (IGFBP) domain, which is as considered as an evolutionarily conserved endocrine longevity assurance pathway[15]. It activates manufacturing and degradation processes in the extracellular matrix and promotes endothelial cell migration and invasion, resulting in the development of new vessels[16-17]. Coumarins are colorless secondary metabolites in higher plants that contain benzopyrene derivatives. They are primarily found in the *Umbelliferae* (also known as *Apiaceae*) family. Antitumor, anti-inflammatory, analgesic, and anti-malarial characteristics are among the biological activities of these substances. Coumarins have a wide range of structural properties, and each one has a unique biological activity based on its chemical structure[18]. Among coumarins, umbelliprenin (UMB) is one of the most well-known coumarin types found in the *Ferula* plant species, *Citrus*, and mountain fennel[19-20]. Many research groups have been interested in UMB during the last decade because of its pharmacological, biological, and phytochemical qualities[21-22]. Gholami *et al*[23] performed a study that demonstrated the anti-inflammatory, antitumor, and anti-angiogenic characteristics of UMB. They discovered that this substance causes an anti-angiogenic impact and reduction of tumor growth. Another study by Mahmoodi Khatonabadi *et al*[24] revealed that UBM could inhibit angiogenesis and metastasis *via* PI3K/Akt/ERK signal pathway in MDA-MB-231 cell line. Another study by these researchers also showed that same signaling pathway
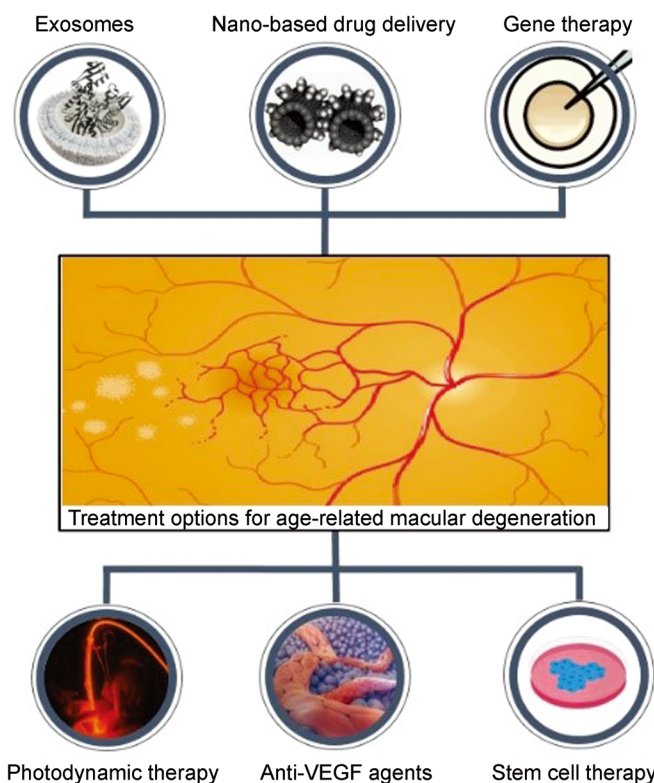

Figure 1 Therapeutic strategies for treating age-related macular degeneration.

could have an anti-angiogenesis impact on the SKBR-3 cell line[25]. Based on these results, we hypothesized that UMB could be an anti-angiogenesis agent for RPE cell line. Although it seems that adjustments are required for efficient transport and delivery, sustaining activity, and increasing the optimal dosage of UMB. For that purpose, we employed a UMB-containing niosome formulation. Niosome (short for non-ionic surfactant-based vesicle) is a type of nano-carrier with significant capacity in encapsulating pharmaceutical agents, both hydrophobic and hydrophilic. They are able to enter the cell by combining with the cell membrane. Niosomes can be categorized into three groups based on the size of the vesicles they contain. These groups include small unilamellar vesicles (SUV) with a size ranging from 0.025 to 0.05 μm, multilamellar vesicles (MLV) with a size larger than 0.05 μm, and large unilamellar vesicles (LUV) with a size greater than or equal to 0.10 μm[26]. Due to the presence of surfactant in its composition, the cell membrane effortlessly merges with niosomes. They also enter the cell by coating the membrane during endocytosis. In general, niosomes have various benefits, including preventing drug inactivation and decomposition, increasing the solubility of water-insoluble and insoluble pharmaceuticals, lowering the drug dose or achieving the correct chemical composition, and increasing the drug's permeability through membranes[27]. Because inhibiting angiogenesis is one of the therapeutical theories for AMD, the goal of this work was to see how the chemical composition of UMB-containing niosome affected
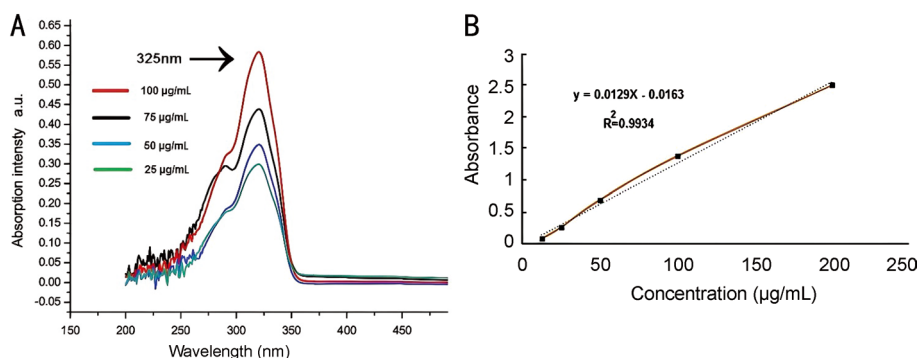
8

Figure 2 UMB characterization and preparation A: The UV-visible spectroscopy of UMB at 325 nm. The concentration of 100 µg/mL of UMB provided the maximum light absorption. B: The standard curve for UMB (R=deviation). UMB: Umbelliprenin; UV: Ultraviolet.

the expression of *VEGF-A* and *CTGF* genes in an RPE-like cell line derived from the human retina. In this study, we evaluated the effects of treating RPE-like retina-derived cell line with free UMB and UMB-containing niosomes nanoparticles on the expression levels of *CTGF* and *VEGF-A* genes.

MATERIALS AND METHODS

Ethical Aproval Our study was approved by Ethics Committee of Golestan University of Medical Science (Ethics Code: IR.GOUMS.REC.1397.268).

Cell Culture The RPE-like cell line was purchased in cryovials (NOYAFAN Inc., Tehran, Iran). After thawing, the cells were grown in T-25 flasks containing a complete culture medium containing 10% fetal bovine serum (FBS) and incubated at 37°C and 5% CO_2. Cell flasks with 90% confluency were used for passage.

Niosome Preparation Four nonionic surfactants (Tween 80, Tween 20, Span 60, Span 20) and cholesterol and drugs were used to synthesize the niosomes by thin-film hydration method. These components were dissolved in 10 mL of the organic solution containing ethanol and chloroform in a 1:1 ratio in a round bottom balloon. A vacuum pump rotary device was used to form a thin film and evaporate organic solvents. The temperature rose to 50°C–60°C. To increase the penetration of the chemical composition of UMB into the lipid membrane of niosomes, the solution was kept at 25°C overnight. The next day, the niosome solution was filtered through a 0.22 nm syringe filter, sonicated for 10min, and stored in the refrigerator.

Determining the Percentage of Encapsulated Drug The concentration of the chemical composition of UMB was analyzed by ultraviolet (UV)-visible spectroscopy to calculate the reference wavelength of UMB (Figure 2A). The standard concentration was selected for the chemical composition of UMB. For that purpose, the light absorption of serially diluted solutions of UMB was measured at the wavelength of 325 nm. Accordingly, the standard curve of the concentration was obtained (Figure 2B). To evaluate the amount of encapsulated drug, 5 mL of the suspension containing nanoparticles was centrifuged at 13 000 prm for 30min. The supernatant

Table 1 Characterization of niosomal nanoparticles size, scattering, and zeta potential

Surfactant	Size (nm)	EE (%)	PDI	Zeta potential
Span 60	110±21.66	75.63±4.59	0.412±0.021	-15.8±0.45
Span 20	94.11±14	61±1.2	0.345±0.035	-11.4±.012
Tween 80	61.34±7.45	45±0.82	0.448±0.011	-4.42±0.56
Tween 20	80.28±12.5	25±0.68	0.387±0.041	-6.25±0.87

EE: Entrapment efficiency; PDI: Polydispersity index.

was washed with 2 mL of PBS buffer. The concentration of the chemical compound in the solution was measured by determining its absorption at 325 nm. The amount of encapsulated drug was calculated using the following formula:

$$Niosome\ EE\% = \frac{Amounts\ of\ drug\ in\ the\ suppernatant}{Total\ amounts\ of\ drug} \times 100$$

Measurement of PDI Size and Zeta Potential Vesicle size, zeta potential, and polydispersity index (PDI) were measured using the dynamic light scattering (DLS) method (Table 1).

***In Vitro* Evaluation of UMB Delivery from Niosome** The delivery rate of UMB from the niosome nanoparticles was measured by the membrane diffusion method. The amount of 2 mL of the niosome solution was poured into a dialysis membrane with a molecular weight cut-off of 10 kDa containing 50 mL of PBS buffer (pH=7.4). It was shacked at 37°C and 40 rpm. At time intervals of 0, 1, 4, 6, 8, 12, and 24h, 2 mL of the solution around the dialysis membrane was removed and replaced with 2 mL of fresh PBS buffer. Then the absorbance of the collected solution was measured at 325 nm. The drug released at each time was calculated using a standard curve, and the drug release was plotted against time.

Analysis of UMB-Containing Niosomes by Infrared Spectroscopy Niosomes were separated from the suspension by centrifugation, and the rest of the solution was evaporated. The samples were suspended in KBr solution and precipitated by centrifugation. The fourier-transform infrared spectroscopy (FT-IR) spectrum was scanned to examine the functional groups of the niosome in the wavelength range of 400–4000 cm^{-1}. The free form was compared to investigate possible chemical interactions between the niosomal system and UMB.

Table 2 Primer sequences used for RT-PCR

Genes	Primers' sequences (5'-3')	Product length	Reference
GAPDH	Forward: 5'-ACAGTCAGCCGCATCTTC-3'	317 bp	
	Reverse: 5'-CTCCGACCTTCACCTTCC-3'		
VEGF-A	Forward: 5'-GGAGGGCAGAATCATCACGAA-3'	3151 bp	Oladnabi *et al*[9]
	Reverse: 5'-GGTCTCGATTGGATGGCAGT-3'		
CTGF	Forward: 5'-TGAAGCTGACCTGGAAGAGA-3'	471 bp	
	Reverse: 5'-GCTCAAACTTGATAGGCTTGG-3'		

RT-PCR: Real-time polymerase chain reaction.

Imaging of UMB-Containing Niosomes Using atomic force microscopy (AFM) and transmission electron microscopy (TEM), the shape and structure of the produced UMB-containing nisomes were examined. For AFM method, a solution of UMB-containing niosomal nanoparticles at a 10 µg/mL concentration was used.

Determining the Optimal Dose of the UMB and Niosomal Nanoparticles The optimal dose was calculated by obtaining the IC50 of the chemical composition of UMB and niosome *in vitro*[28]. In this regard, 35 000 RPE cells were counted and seeded onto the 96-well plates. After a 24-hour incubation, the cells were treated with different doses of UMB or UMB-containing niosome. Each test was repeated three times. After 24, 48, and 72h of treatment, the 3-(4,5-dimethylthiazol-2-yl)-2,5-diphenyltetrazolium bromide (MTT) assay was used to evaluate cell survival as described before[29]. After the formation, purple crystals of formazan were dissolved in DMSO. Light absorption was measured at 570 nm using an ELISA reader.

RNA Extraction, cDNA Synthesis, and Real-Time PCR According to the kit instructions (DenaZist, Iran), RNA extraction was performed from 2–4×10^5 RPE cells treated with UMB or UMB-containing niosome. The NanoDrop device measured the purity of extracted RNA. The ratio of 260/280 and 260/230 optical densities (OD) between 1.8 and 2 was considered pure extracted RNA. The extracted RNA was used to synthesize cDNA according to the kit instructions (Pars Toos, Iran). Internal glyceraldehyde 3-phosphate dehydrogenase (*GAPDH*) control was used to evaluate RNA extraction and cDNA synthesis. Real-time polymerase chain reaction (RT-PCR) evaluated the expression of *VEGF-A*, *CTGF*, and *GAPDH* genes[30]. The PCR primers that were obtained from our previous work are listed in Table 1[9]. Required materials and thermal cycles were used according to the kit instructions (Table 2).

Statistical Analysis The results of RT-PCR were calculated by the $2^{-\Delta\Delta Ct}$ method. The expression of *VEGF-A* and *CTGF* genes was compared with the *GAPDH* gene expression in different cell groups. GraphPad Prism software was used to generate the graphs. Also, the Student's *t*-test with a 95% confidence level was used to evaluate the gene expression differences due to the chemical combination of UMB and UMB-containing niosomal nanoparticles. A *P*-value less than 0.05 was considered significant.

RESULTS

Niosomes Characterization UMB-containing niosomes were fabricated. The amount of trapping of UMB compound by niosomes with Span 60, Span 20, Tween 20, Tween 80 surfactants was 75.63%±4.59%, 61%±1.2%, 25%±0.68%, 45%±0.82%, respectively. Niosomes made with non-surfactant Span 60 had the highest entrapment efficiency (EE). Niosomes formulations with cholesterol: Span 60 ratio of 0:1, 0.5:1, 1:1, and 2:1 had EEs of 15.24%±0.5%, 24.33%±1.68%, 75.63%±4.59%, and 58.32%±1.8%, respectively (Figure 3A). Niosomes size ranged from 61±7.45 nm to 110±21.66 nm (Figure 3B). The dispersion index for all four formulations prepared was less than 0.5 (PDI<0.5). This indicates the comparable size of the niosomes and their low tendency to aggregate with each other.

***In Vitro* Delivery of UMB from the Niosome** The amount of UMB released from the niosomes in phosphate buffer during time intervals of 0, 1, 4, 6, 8, 12, and 24h was calculated using the standard calibration curve. The 62.35% of the chemical composition of UMB within the structure of the niosome was released during the first 4h of incubation (Figure 3C). According to the FT-IR spectrum, the composition of the UMB of the indices peak of 1680 cm^{-1}, 1730 cm^{-1}, and 2810 cm^{-1} were observed (Figure 4A). The peak of 1680 cm^{-1} is characteristic of the aromatic alkene group, and the peak of 1730 cm^{-1} is characteristic of the ester group (CO, it's for carbon and oxygen) in the chemical composition of UMB. The 1180 cm^{-1} was the characteristic of ether CO group in Span 60, and peak 1680 cm^{-1} characteristic of aromatic alkene group in UMB. Peaks at 1730 cm^{-1}, 2430 cm^{-1}, and 2810 cm^{-1} were distinct CO ester groups of UMB in niosomes (Figure 4B). The peaks at 1180 cm^{-1} and 2430 cm^{-1} were characteristic of the ether CO group in Span 60. Since no new peak has been observed, it seems that no interaction has occurred between UMB and niosomes, and the encapsulation process didn't change the UMB structure.

Imaging of UMB-Containing Niosomes Using AFM and TEM microscopy, the surface morphology of the niosomes that contain the chemical composition of UMB was determined (Figure 5).
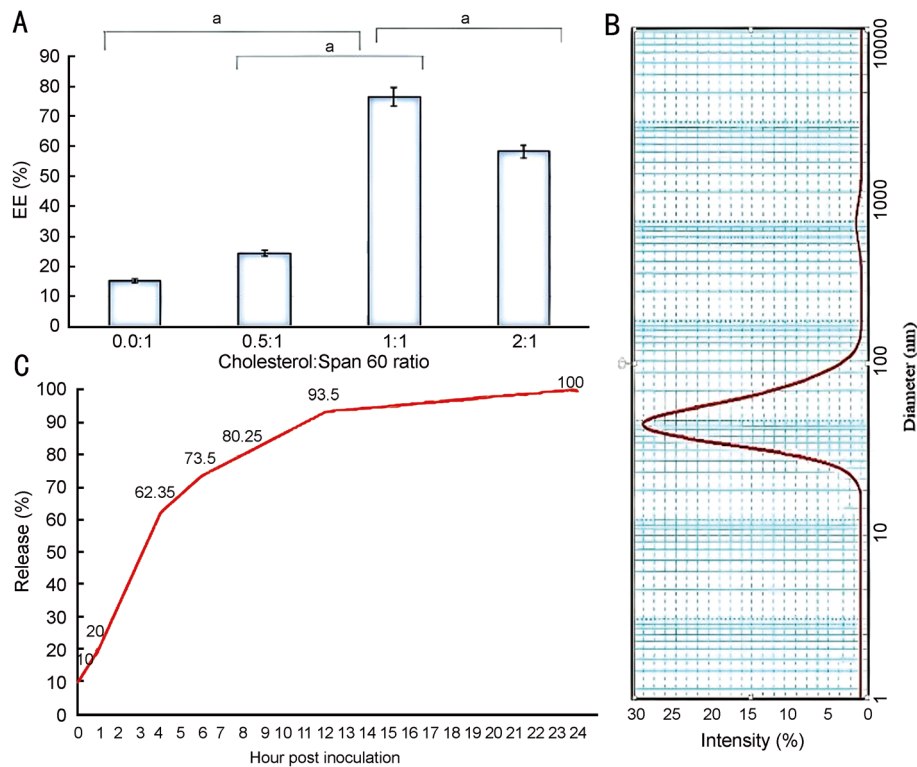
Figure 3 Niosomes characteristics A: Maximum UMB uptake by niosomes was achieved at 1:1 cholesterol-Span 60 ratio; B: Dynamic light scattering diagrams of UMB-containing niosomes; C: The release of UMB from niosomal nanoparticles is referred to time interval. UMB: Umbelliprenin. [a]$P<0.05$.
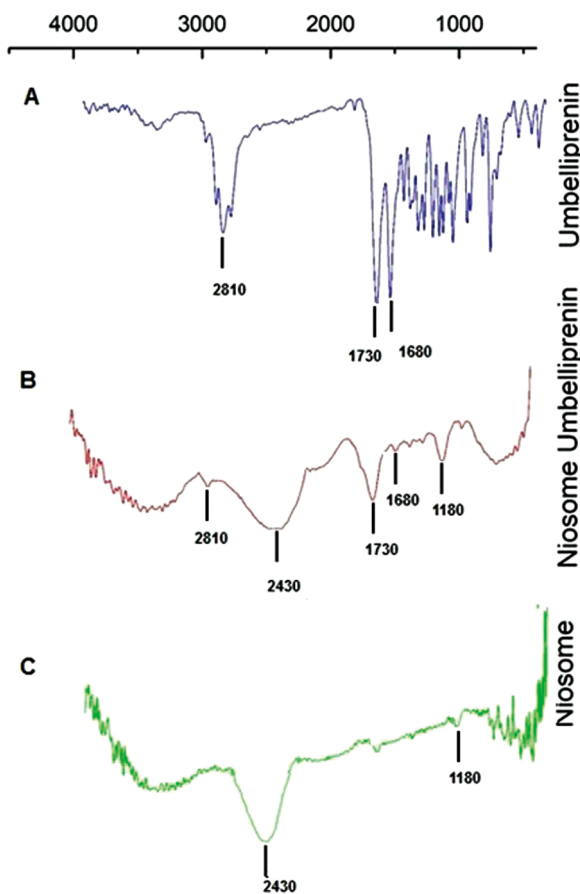

Figure 4 Fourier-transform infrared spectroscopy spectrum of free niosome (A), free UMB (B), and UMB-containing niosomes (C) UMB: Umbelliprenin.
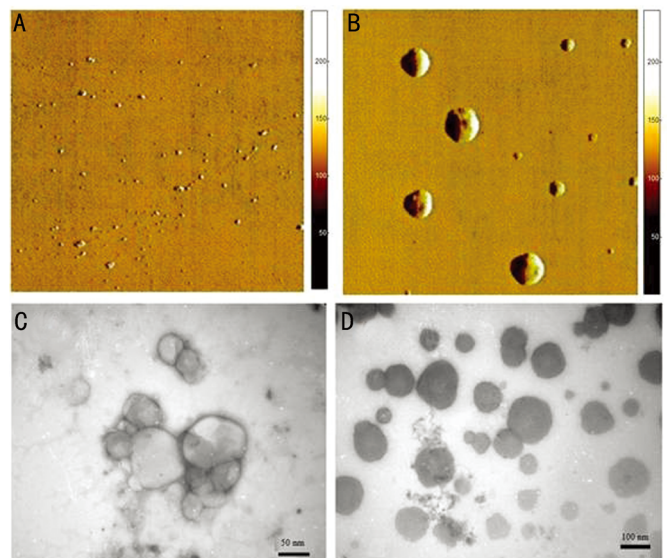

Figure 5 Atomic force microscopy (A and B) and transmission electron microscopy (C and D) images of UMB-containing niosomes UMB: Umbelliprenin.

Cell Viability Cell viability was assessed on RPE cells treated with UMB at eight concentrations of 3, 6, 12, 25, 50, 75, 100, and 200 μg/mL at 3 time intervals of 24, 48, and 72h by MTT assay. All tests were repeated three times. The results of each sample were compared with controls. In addition, an MTT assay was performed on RPE cells treated with UMB-containing niosome at eight concentrations of 3, 6, 12, 25, 50, 75, 100, and 200 μg/mL at three times 24, 48, and 72h. It was
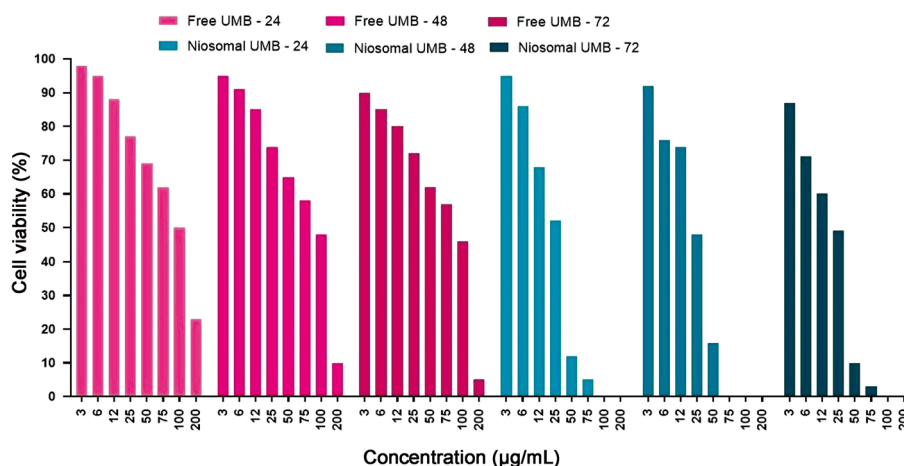
Figure 6 MTT assay of free and niosome-capsulated UMB MTT: 3-(4,5-dimethylthiazol-2-yl)-2,5-diphenyltetrazolium bromide; UMB: Umbelliprenin.
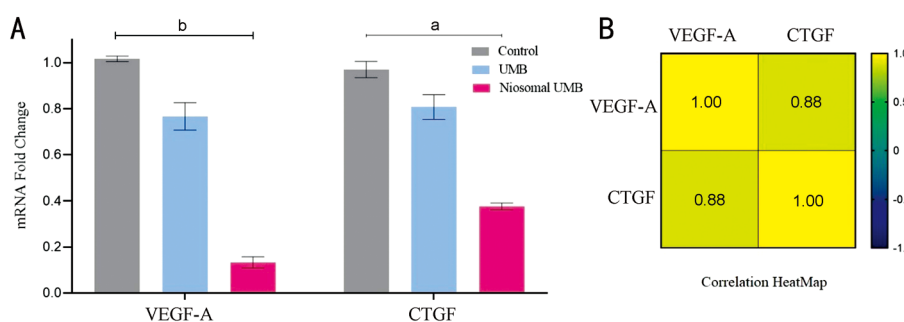

Figure 7 Gene expression analysis A: Results of gene expression level from cells 24h after treating with free UMB and niosome-encapsulated UMB; B: Spearman's rank correlation coefficients of *VEGF-A* and *CTGF* expression in RPE-like cells treated with UMB; -1 and 1 indicate perfect negative and positive correlations, respectively. UMB: Umbelliprenin. [a]$P<0.05$; [b]$P<0.001$.

initially found that the toxicity of UMB-containing niosomes is significantly higher than free UMB. It was also found that the drug's toxicity in niosomal formulations was higher than the free drug—both free and encapsulated UMB reduced cell survival at different doses and times. Studies have shown that the toxicity of UMB-containing niosome is significantly higher than free UMB. To find the optimal dose (IC50) of the free UMB, MTT test results were evaluated in all 3 time periods of 24, 48, and 72h. The IC50 of UMB was 100, 96.2, and 94.1 µg/mL for 24h, 48h, and 72h post-inoculation time, respectively. These results showed that the effect of free UMB on the RPE-like cell line is dose-dependent but not time-dependent (Figure 6). Also, MTT test results were evaluated in all three time periods of 24, 48, 72h to obtain the optimal dose of UMB-containing niosome. The IC50 of UMB-containing niosome for 26, 48, and 72h post-inoculation was 26, 23, and 24 µg/mL, respectively. Because 63.35% of the encapsulated UMB was released from the capsule in the first 4h and according to the MTT results of UMB-containing niosome, UMB also had dose-dependent toxicity.

Gene Expression of *VEGF-A* and *CTGF* The effect of free UMB and UMB-containing niosome on the expression of *VEGF-A* and *CTGF* genes was investigated in RPE-like cells using RT-PCR. The results (Figure 7A) showed that treatment with both free UMB and UMB-containing niosome did not lead to a significant decrease in the expression of *VEGF-A* or *CTGF* compared to the control group. However, treatment with UMB-containing niosome resulted in a significantly greater decrease in *VEGF-A* expression than free UMB ($P<0.001$), and a significant decrease in *CTGF* expression ($P<0.05$). We also computed the Spearman's rank correlation coefficient between the *VEGF-A* and *CTGF* and obtained a value of 0.883 with P value of 0.003 (Figure 7B), which means that these two genes have a positive correlation in cultured RPE-like cells treated with UMB.

DISCUSSION

To date, various therapeutic approaches have been proposed for AMD disease. Based on the occurrence of angiogenesis behind the retina, the disease is divided into two categories: nonexudative or dry AMD and exudative neovascular or wet AMD[3]. *VEGF-A* and *CTGF* are recognized as two essential factors with positive regulatory effects on the development of pathological angiogenesis. Studies have shown that inhibiting *VEGF-A* and *CTGF* genes in retinal cells can be effective in reducing neovascularization, edema, and fibrosis in animal models of diabetic retinopathy (DR)[31]. Inhibition of both
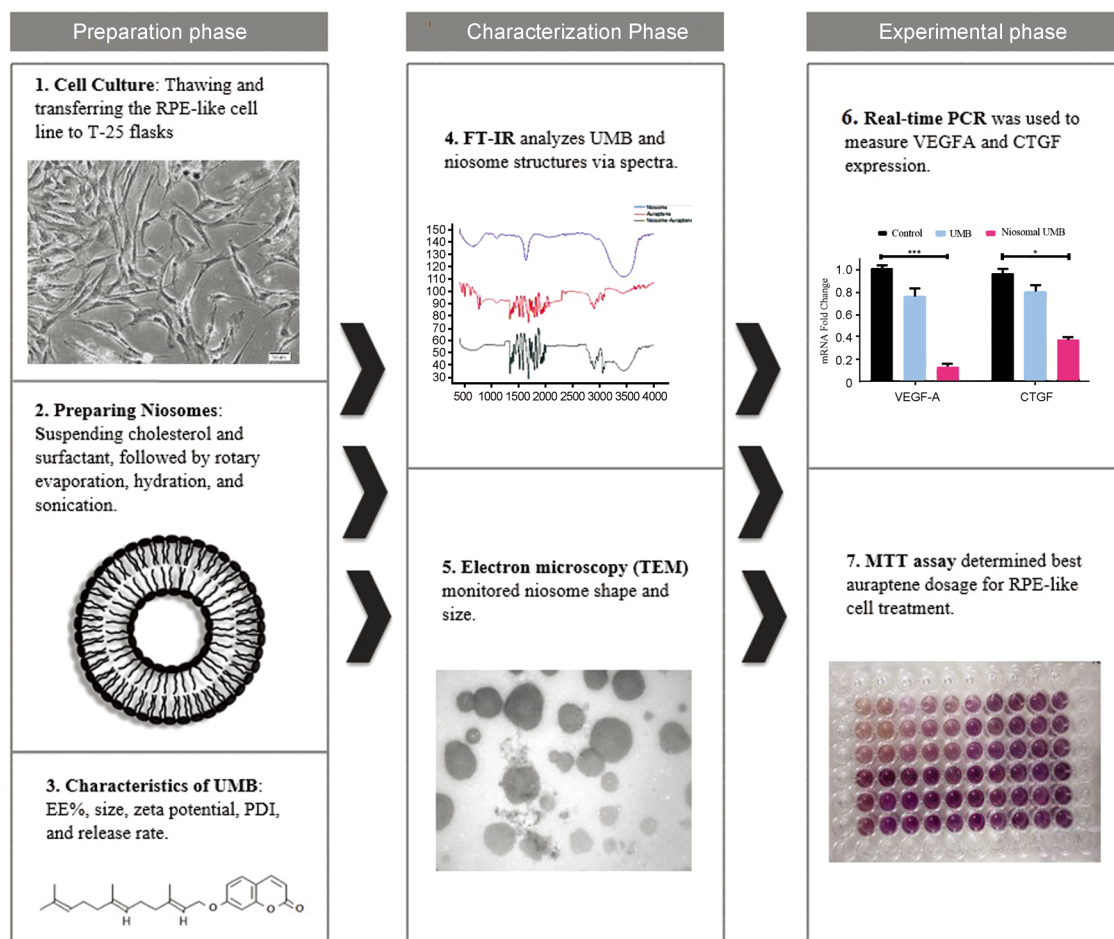
Figure 8 The graphical abstract shows the workflow of the study divided into three main phases: preparation, characterization, and *in-vitro* experimental UMB: Umbelliprenin; RPE: Retinal pigment epithelium; VEGF: Vascular endothelial growth factor; CTGF: Connective tissue growth factor; RT-PCR: Real-time polymerase chain reaction; FT-IR: Fourier-transform infrared spectroscopy; MTT: 3-(4,5-dimethylthiazol-2-yl)-2,5-diphenyltetrazolium bromide.

VEGF-A and *CTGF* is helpful in the treatment of AMD[12-17]. In fact, many attempts have been made recently to treat AMD using angiogenesis inhibitors. Although most studies are focused on pegaptanib, ranibizumab, and bevacizumab, they haven't had much success in AMD therapeutics. Therefore, new studies should be focused on more effective angiogenesis inhibitors[32-34]. Coumarins are naturally derived from benzopyrenes found in a variety of plants. They have a well-established role in biological processes against tumors, malaria, and inflammation[35]. Many species of the *Ferula* plant synthesize coumarins. One type of coumarin is UMB. It is the first discovered coumarin synthesized in the *Ferula*. Recent studies have shown a wide range of clinical benefits of UMB, including anti-inflammatory, anti-cytotoxic, detoxifying, and antitumor properties[22-25]. For instance, a recent study by Naderi Alizadeh *et al*[36] has demonstrated that UMB has antitumor effects by substantially reducing VEGF, MMP2, and MMP-9 levels *in vivo*. Here in this study (Figure 8), we investigated the anti-AMD activity of UMB. In order to enhance the durability of UMB activity, it was decided to

formulate it on a non-ionic nanoparticle. Nanoparticles are advantageous to increase the continuity of drug delivery and preserving the therapeutic compounds from degradation. Non-ionic nanoparticles like niosome create a substrate for gradually trapping the chemical compound, enhancing the durable biological activity. In the present study, it was found that formulations containing Span had higher EE than formulations containing Tween. This could be due to the hydrophilicity to hydrophobicity (HLB) ratio of non-ionic surfactants. A formulation containing Span 60 had the highest EE (75.63%), while a formulation containing Tween 80 had the lowest EE (25%). Our findings were consistent with the study by Bayindir and Yuksel[37]. After selecting the nonionic surfactant Span 60, different ratios of surfactant to cholesterol (1:1, 0.5:1, 0:1) were examined. The results showed that the 1:1 formulation of surfactant to cholesterol had the highest EE. Reducing the ratio of cholesterol to surfactant prevented the proper formation of a thin film. Increasing the ratio of cholesterol to surfactant decreased the EE, which could be due to the competition between cholesterol and the hydrophobic

composition of UMB to be placed in a bilayer membrane. This was consistent with the results of the study by Abdelbary and El-gendy[38]. The results of RT-PCR showed that the chemical composition of free-state UMB and the UMB-containing niosome both reduced the expression of the *VEGF-A* and *CTGF* genes. In addition, UMB-containing niosome had a more significant effect on reducing *VEGF-A* and *CTGF* genes than free UMB. This might be due to the higher reduction in gene expression with lower doses of UMB. These results indicate that UMB is a chemical with anti-*VEGF* and anti-*CTGF* properties and can be anti-angiogenic either freely or in combination with niosome. Our results demonstrate that UMB on the niosomes nanoparticles is a promising therapeutic option for AMD. The molecular mechanism by which UMB will exert its effect on AMD by reducing angiogenesis-related factors like *VEGF-A* and *CTGF* is not completely clear and necessitates more studies in the future.

In conclusion, UMB is an effective anti-angiogenesis chemical. Niosomes nanoparticles enhance the angiogenesis inhibitory ability of UMB. The anti-angiogenesis activity of the complex of niosomes and UMB decreased the expression of *VEGF-A* and *CTGA* genes. This implicates that UMB-containing niosomes can also be used to study their therapeutics effect on other angiogenesis-dependent diseases.

ACKNOWLEDGEMENTS

REFERENCES

1 Wong WL, Su X, Li X, Cheung CM, Klein R, Cheng CY, Wong TY. Global prevalence of age-related macular degeneration and disease burden projection for 2020 and 2040: a systematic review and meta-analysis. *Lancet Glob Health* 2014;2(2):e106-e116.

2 Pennington KL, DeAngelis MM. Epidemiology of age-related macular degeneration (AMD): associations with cardiovascular disease phenotypes and lipid factors. *Eye Vis (Lond)* 2016;3(1):1-20.

3 Lim LS, Mitchell P, Seddon JM, Holz FG, Wong TY. Age-related macular degeneration. *Lancet* 2012;379(9827):1728-1738.

4 Han Y, Yang KH, He DX, *et al*. Effect of palmitoylethanolamide on degeneration of a human-derived retinal pigment epithelial cell induced by all-trans retinal. *Int J Ophthalmol* 2023;16(2):191-200.

5 DeAngelis MM, Owen LA, Morrison MA, *et al*. Genetics of age-related macular degeneration (AMD). *Hum Mol Genet* 2017;26(R1):R45-R50.

6 Vanderbeek BL, Zacks DN, Talwar N, Nan B, Musch DC, Stein JD. Racial differences in age-related macular degeneration rates in the United States: a longitudinal analysis of a managed care network. *Am J Ophthalmol* 2011;152(2):273-282.e3.

7 Kauppinen A, Paterno JJ, Blasiak J, Salminen A, Kaarniranta K. Inflammation and its role in age-related macular degeneration. *Cell Mol Life Sci* 2016;73(9):1765-1786.

8 Nita M, Grzybowski A. The role of the reactive oxygen species and oxidative stress in the pathomechanism of the age-related ocular diseases and other pathologies of the anterior and posterior eye segments in adults. *Oxidative Med Cell Longev* 2016;2016:1-23.

9 Oladnabi M, Bagheri A, Rezaei Kanavi M, Azadmehr A, Kianmehr A. Extremely low frequency-pulsed electromagnetic fields affect proangiogenic-related gene expression in retinal pigment epithelial cells. *Iran J Basic Med Sci* 2019;22(2):128-133.

10 Oladnabi M, Amir Mishan M, Rezaeikanavi M, Zargari M, Najjar Sadeghi R, Bagheri A. Correlation between ELF-PEMF exposure and human RPE cell proliferation, apoptosis and gene expression. *J Ophthalmic Vis Res* 2021;16(2):202-211.

11 Holmes DIR, Zachary I. The vascular endothelial growth factor (VEGF) family: angiogenic factors in health and disease. *Genome Biol* 2005;6(2):209.

12 Amoaku WM, Chakravarthy U, Gale R, *et al*. Defining response to anti-VEGF therapies in neovascular AMD. *Eye (Lond)* 2015;29(6):721-731.

13 Kim BH, Yu HG, Hong IH. Volumetric fluid analysis of fixed monthly anti-VEGF treatment in patients with neovascular age-related macular degeneration. *Int J Ophthalmol* 2023;16(6):909-914.

14 Rubner R, Valeria Canto-Soler M. Progress of clinical therapies for dry age-related macular degeneration. *Int J Ophthalmol* 2022;15(1):157-166.

15 Ungvari Z, Valcarcel-Ares MN, Tarantini S, Yabluchanskiy A, Fülöp GA, Kiss T, Csiszar A. Connective tissue growth factor (CTGF) in age-related vascular pathologies. *Gero Science* 2017;39(5):491-498.

16 Mongiat M, Andreuzzi E, Tarticchio G, Paulitti A. Extracellular matrix, a hard player in angiogenesis. *Int J Mol Sci* 2016;17(11):E1822.

17 Bagheri A, Soheili ZS, Ahmadieh H, *et al*. Simultaneous application of bevacizumab and anti-CTGF antibody effectively suppresses proangiogenic and profibrotic factors in human RPE cells. *Mol Vis* 2015;21:378-390.

18 Hussain MI, Syed QA, Khattak MNK, Hafez B, Reigosa MJ, El-Keblawy A. Natural product coumarins: biological and pharmacological perspectives. *Biologia* 2019;74(7):863-888.

19 Ding AJ, Zheng SQ, Huang XB, Xing TK, Wu GS, Sun HY, Qi SH, Luo HR. Current perspective in the discovery of anti-aging agents from natural products. *Nat Prod Bioprospect* 2017;7(5):335-404.

20 Shakeri A, Iranshahy M, Iranshahi M. Biological properties and molecular targets of umbelliprenin—a mini-review. *J Asian Nat Prod Res* 2014;16(8):884-889.

21 Fiorito S, Preziuso F, Sharifi-Rad M, Marchetti L, Epifano F, Genovese S. Auraptene and umbelliprenin: a review on their latest literature acquisitions. *Phytochem Rev* 2022;21(2):317-326.

22 Shahzadi I, Ali Z, Baek SH, Mirza B, Ahn KS. Assessment of the antitumor potential of umbelliprenin, a naturally occurring sesquiterpene coumarin. *Biomedicines* 2020;8(5):126.

23 Gholami O, Jeddi-Tehrani M, Iranshahi M, Zarnani AH, Ziai SA. Mcl-1 is up regulated by prenylated coumarin, umbelliprenin in jurkat cells. *Iran J Pharm Res* 2014;13(4):1387-1392.

24 Mahmoodi Khatonabadi S, Salami S, Mirfakhraie R, *et al*. Umbelliprenin inhibited angiogenesis and metastasis of MDA-MB-231 cell line through downregulation of CoCl$_2$/EGF-mediated PI3K/AKT/ERK signaling. *Middle East J Cancer* 2022;13(2):226-236.

25 Atabakhshian R, Salami S, Mirfakhraie R, *et al*. Umbelliprenin suppresses angiogenesis signaling in SKBR-3 cell line by downregulation of EGF/CoCl$_2$ -mediated PI3K/AKT/MAPK. *Res J Pharmacogn* 2021;8(1):7-18.

26 Kuotsu K, Karim K, Mandal A, Biswas N, Guha A, Chatterjee S, Behera M. Niosome: a future of targeted drug delivery systems. *J Adv Pharm Tech Res* 2010;1(4):374.

27 Ge XM, Wei MY, He SN, Yuan WE. Advances of non-ionic surfactant vesicles (niosomes) and their application in drug delivery. *Pharmaceutics* 2019;11(2):55.

28 Mohebbi A, Azadi F, Hashemi MM, Askari FS, Razzaghi N. Havachoobe (*Onosma dichroanthum boiss*) root extract decreases the hepatitis B virus surface antigen secretion in the PLC/PRF/5 cell line. *Intervirology* 2021;64(1):22-26.

29 Mohebbi A, Ebrahimzadeh MS, Baghban Rahimi S, *et al*. Non-replicating Newcastle Disease Virus as an adjuvant for DNA vaccine enhances antitumor efficacy through the induction of TRAIL and granzyme B expression. *Virus Res* 2019;261:72-80.

30 Mohebbi A, Mamizadeh Z, Bagheri H, Sharifnezhad F, Tabarraei A, Yazdi M. Prevalent latent human cytomegalovirus genotype b2 in biopsy samples of gastric cancer. *Future Virol* 2020;15(2):71-78.

31 Estrada CC, Maldonado A, Mallipattu SK. Therapeutic inhibition of VEGF signaling and associated nephrotoxicities. *J Am Soc Nephrol* 2019;30(2):187-200.

32 Nowak JZ. Age-related macular degeneration (AMD): pathogenesis and therapy. *Pharmacol Rep* 2006;58(3):353-363.

33 Ferrara N. Vascular endothelial growth factor and age-related macular degeneration: from basic science to therapy. *Nat Med* 2010;16(10):1107-1111.

34 Rastoin O, Pagès G, Dufies M. Experimental models in neovascular age related macular degeneration. *Int J Mol Sci* 2020;21(13):4627.

35 Menezes JC, Diederich M. Translational role of natural coumarins and their derivatives as anticancer agents. *Future Med Chem* 2019;11(9):1057-1082.

36 Naderi Alizadeh M, Rashidi M, Muhammadnejad A, Moeini Zanjani T, Ziai SA. Antitumor effects of umbelliprenin in a mouse model of colorectal cancer. *Iran J Pharm Res* 2018;17(3):976-985.

37 Bayindir ZS, Yuksel N. Characterization of niosomes prepared with various nonionic surfactants for paclitaxel oral delivery. *J Pharm Sci* 2010;99(4):2049-2060.

38 Abdelbary G, El-gendy N. Niosome-encapsulated gentamicin for ophthalmic controlled delivery. *AAPS Pharmscitech* 2008;9(3):740-747.